JMEPEG (2002) 11:537–543

Hot Tearing Studies in AA5182

W.M. van Haaften, W.H. Kool, and L. Katgerman

(Submitted 26 April 2002)

One of the major problems during direct chill (DC) casting is hot tearing. These tears initiate during solidification of the alloy and may run through the entire ingot. To study the hot tearing mechanism, tensile tests were carried out in semisolid state and at low strain rates, and crack propagation was studied in situ by scanning electron microscopy (SEM). These experimentally induced cracks were compared with hot tears developed in an AA5182 ingot during a casting trial in an industrial research facility. Similarities in the microstructure of the tensile test specimens and the hot tears indicate that hot tearing can be simulated by performing tensile tests at semisolid temperatures. The experimental data were compared with existing hot tearing models and it was concluded that the latter are restricted to relatively high liquid fractions because they do not take into account the existence of solid bridges in the crack.

Keywords AA5182 ingot, DC casting, hot tearing, tensile tests

1. Introduction

During direct chill (DC) casting of aluminum (Al) alloys, the primary and secondary cooling cause strong thermal gradients in the ingot that may lead to distortion of the ingot shape (e.g., butt curl, butt swell, rolling face pull-in) and/or to hot tearing and cold cracking. This study focuses on one of these problems: hot tearing.

From many studies[1-9] starting as early as the 1950s and reviewed in Ref. 10, it appears that hot tears initiate above the solidus temperature and propagate in the interdendritic liquid film. This results in a bumpy crack surface covered with a smooth layer and sometimes with solid bridges, which connect both sides of the crack.[8,9,11-17] During solidification, the liquid flow through the mushy zone decreases until it becomes insufficient to fill initiated cavities, which allows the cavities to grow further. The solidification process can be divided in four stages, based on the permeability of the solid network:[3,6,9,18] (1) mass feeding, in which both liquid and solid are free to move; (2) interdendritic feeding, in which the remaining liquid has to flow through the dendritic network; (3) interdendritic separation, in which the liquid network becomes fragmented and pore formation or hot tearing may occur; and (4) interdendritic bridging or solid feeding, in which the ingot has developed a considerable strength and further shrinkage is compensated by solid-state creep. A large freezing range of the alloy promotes hot tearing because these alloys spend a long time in the vulnerable state in which thin liquid films exist between the dendrites. The liquid film distribution is determined by the dihedral angle θ. With a low dihedral angle, the liquid will tend to spread out over the grain boundary surface, which strongly reduces the dendrite coherency. With a high dihedral angle the liquid will remain as droplets at the triple points so that the solid network holds its strength.

W.M. van Haaften, W.H. Kool, and **L. Katgerman,** Laboratory of Materials, Delft University of Technology, Rotterdamseweg 137, 2628 AL Delft, The Netherlands. Contact e-mail: L.Katgerman@tnw.tudelft.nl.

Apart from these intrinsic factors, the solidification shrinkage and thermal contraction impose strains and stresses on the solid network, which are required for hot tearing. It is argued that it is mainly the strain and the strain rate that are critical for hot tearing.[2,9] Stresses do not seem critical because the forces available during solidification are very high compared with the stresses a semisolid network can resist.[9]

Several hot tearing criteria have been developed in the past decades. Feurer[5] used the fluid flow through a porous network to calculate the afterfeeding by liquid metal. Hot tears will initiate when this afterfeeding cannot compensate the solidification shrinkage. Clyne and Davies[6] defined a cracking susceptibility coefficient (CSC) as the ratio between the time, t_V, during which the alloy is prone to hot tearing and the time, t_R, during which stress relaxation and afterfeeding can take place. These times are defined as the periods during which the fraction liquid is between 0.1 and 0.01 and between 0.1 and 0.6, respectively. These criteria were combined with a heat flow model describing the DC casting process by Katgerman.[19] This enabled the determination of the cracking susceptibility coefficient as a function of the casting parameters. Unfortunately, the above criteria are restricted in their use because they give only a qualitative indication for the hot tearing susceptibility.

The first two-phase model, which takes into account both fluid flow and deformation of the solid network, is the Rappaz-Drezet-Gremaud (RDG) hot tearing criterion.[20] The RDG criterion is formulated on the basis of afterfeeding, which is limited by the permeability of the mushy zone. At the solidification front the permeability is high, but deeper in the mushy zone the permeability is restricted. A pressure drop along the mushy zone exists that is a function of this permeability and the strain rate. If the local pressure becomes lower than a critical pressure, a cavity is initiated. The model is implemented in a thermomechanical model for DC casting by Drezet et al.[21] to predict hot tearing during billet casting. The hot tearing susceptibility is found to be higher during startup of the casting and in the center of the billet, which agrees with general casting practice.

An additional development of the RDG criterion is carried out by Braccini et al.[22] They included plastic deformation of

the solid phase and a criterion for the growth of a cavity. They based their model on two simplified geometric models, one for a columnar dendritic structure and one for an equiaxed dendritic structure. Explicit relations are developed for critical strain rates and they indicate that the critical strain rate decreases with increasing solid fraction.

Many studies have used tensile testing at semisolid temperatures to study hot tearing either by in situ solidification experiments[11-13,18,23-25] or by reheating specimens from room temperature.[15,24,26-28] Both techniques led to the following general results. In several Al alloys, it is observed that both strength and ductility strongly decrease from just below the solidus temperature to the semisolid state, whereas the fracture surface changes from rough, related to the ductile behavior, to smooth, related to the presence of a liquid film. Furthermore, cracks initiate at micropores or molten inclusions and continue along grain boundaries.

The prediction of hot tears during DC casting is complicated because of the complex cooling conditions and subsequent development of thermal stresses. Models developed for this purpose require a detailed knowledge of the process conditions and hot tearing mechanisms. Therefore, a microstructural investigation of hot tearing in an AA5182 alloy was carried out in two ways: tensile specimens were deformed at various temperatures above the solidus and under different loads, which for certain conditions led to fracture. Furthermore, crack propagation was studied in situ at 500 °C. In both cases, the fracture surfaces of the specimens were investigated by scanning electron microscopy (SEM). The results of the tests were compared with a hot tearing surface in an industrial AA5182 ingot and current hot tearing criteria were evaluated.

2. Experimental

2.1. Material

The material investigated is an AA5182 alloy. It was sampled from a rolling slab, which was DC cast at an industrial research facility. The composition in wt.% was Mg, 3.6; Mn, 0.16; Si, 0.21; Fe, 0.26; Al, bal. The slab was not heat treated.

2.2. Tensile Tests

The experiments were carried out with a Gleeble 3500 thermomechanical simulator (Duffers Inc., Poestenkill, NY). The specimens with the same shape as reported earlier[29] were tested with their tensile direction parallel to the casting direction. They were heated as fast as possible (50 °C/s) by Joule heating to the semisolid temperature to minimize changes in the as-cast structure, and under argon atmosphere to prevent oxidation of the fracture surface. The tensile tests were carried out in force control and at low strain rate ($<3 \times 10^{-3}$ s^{-1}). At the moment the force was seen to decrease, which was interpreted as crack initiation, the specimen was quenched with water to preserve the microstructure at the time of fracture. Nonfractured specimens were quenched immediately after the tensile test. The material was tested at temperatures from 500-580 °C and at stress levels between 0.8 and 10 MPa. The fraction liquid was calculated with the Alstruc model.[30-32] After the tests, selected nonfractured specimens were cut parallel to the tensile direction and studied by optical microscopy. The grain size was determined with the line interception method. Fractured specimens were studied by SEM.

2.3. In Situ Cracking Observation

In a SEM equipped with a hot stage, polished flat specimens with a V-notch (Fig. 1) were heated and deformed in

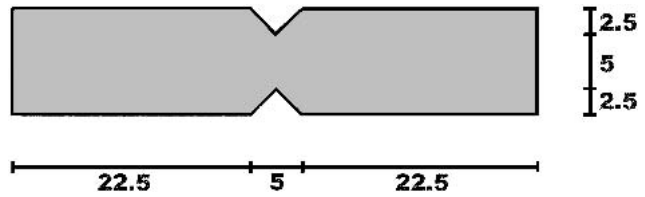

Fig. 1 Schematic drawing of specimen used for in situ observations. Dimensions are in mm. Thickness is 1.5 mm.

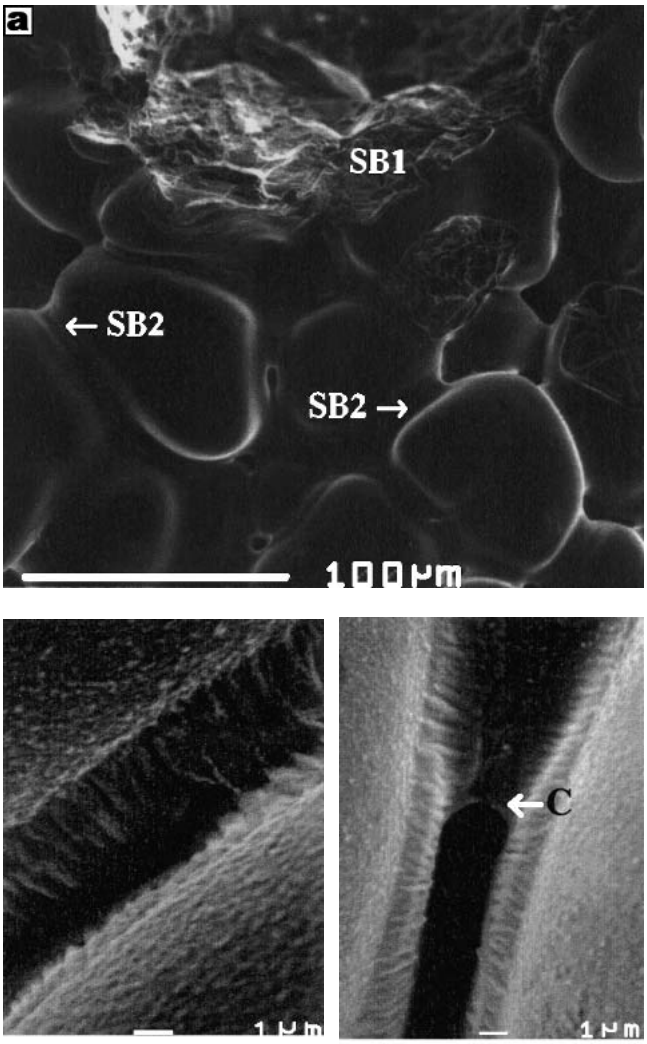

Fig. 2 SEM micrograph of fracture surface of tensile specimen, fractured at 560 °C. **(a)** Grains covered with a (solidified) liquid film. SB1, remains of fractured solid bridges; SB2, solid bridge still intact. **(b)** Side crack, not fully separated. **(c)** Separated grains with some remaining liquid which forms a capillary meniscus (C)

tension. The specimen was mounted on a heating element and heated to 500 °C in 2 min. The specimen was then deformed at a speed of 0.2 μm/s and crack propagation was studied. The tensile direction was normal to the casting direction and parallel to the rolling face of the slab.

2.4. Observation of Hot Tear Surface in an Industrial Ingot

Samples from casting experiments with AA5182 at an industrial research facility were selected and hot tears were investigated by SEM. The location of the samples was in the steady-state part of the ingot at circa 10 cm from the crack initiation point. The samples were etched to remove the oxide layer on the hot tearing surface.

3. Results

3.1. Tensile Tests and Microstructural Observations

The resulting strain rate and strain of the tensile tests are summarized in Table 1. Also indicated are the liquid fraction f_L and whether the specimen fractured.

Optical microscopy on the uncracked specimens and on an as-cast specimen showed that all specimens had a similar grain size (110-120 μm), had Al_6 (Mn, Fe) and Al_3Mg_2 as constituent particles, and contained some porosity. No crack initiation phenomena were observed in the strained specimens. Thus, no major differences between the strained specimens themselves or with the as-cast specimen were observed.

SEM observations were made of the fracture surface of the specimen fractured at 560 °C and $\varepsilon = 0.005$. Figure 2 shows grains, which are covered with a smooth layer that was liquid at the time of fracture. Where the gap between two grains became too large, holes developed in the liquid film. In some parts, the two crack sides were still connected by solid bridges, which are solid connections between dendrite arms. Evidence for this is seen in the rough surface in Fig. 2 at location SB1 where solid-state rupture has taken place. Solid bridges still in place are also present, as can be seen at location SB2. Figure 2(b) shows in detail one of the many side cracks in its final stage before decohesion. It is partly filled with solidified liquid. Figure 2(c) shows two separated grains with some remaining liquid. In this case, the liquid metal pressure was not high enough to feed the entire crack and a capillary meniscus remained.

Table 1 Experimental Parameters for the Hot Tearing Simulations With AA5182 and Resulting Strain Rate and Strain

T, °C	f_L	σ, MPa	$\dot{\varepsilon}$, s^{-1}	ε	Remark
500	0.00	8	2.7×10^{-4}	0.005	
500	0.00	8	3.3×10^{-4}	0.016	
510	0.00	4	4.4×10^{-5}	0.007	
510	0.00	8	2.1×10^{-4}	0.020	
520	0.01	6	1.5×10^{-4}	0.004	
520	0.01	3	8.2×10^{-5}	0.006	
530	0.02	3	4.8×10^{-5}	0.006	
540	0.02	4	1.9×10^{-4}	0.004	
540	0.02	4	2.5×10^{-4}	0.004	
540	0.02	2	5.2×10^{-5}	0.006	
540	0.02	10	2.5×10^{-3}	0.013	Cracked
540	0.02	10	2.7×10^{-3}	0.014	
550	0.03	1	3.3×10^{-5}	0.004	
550	0.03	3	1.6×10^{-4}	0.004	
550	0.03	5	8.0×10^{-4}	0.008	Cracked
556	0.04	3	1.5×10^{-4}	0.002	
560	0.04	2	9.0×10^{-4}	0.001	Cracked
560	0.04	2	6.5×10^{-4}	0.005	Cracked
580	0.07	0.8	5.0×10^{-4}	0.003	Cracked
580	0.07	0.8	3.3×10^{-4}	0.005	Cracked
580	0.07	0.9	4.0×10^{-4}	0.010	Cracked

3.2. In Situ Cracking Observation

Figure 3 shows two still photographs from the video of the in situ deformation in the SEM at 500 °C. The crack started at the notch of the specimen, but after some deformation, cracks also initiated at grain boundaries and pores. These separate cracks grew to each other to form the final crack. They mainly followed the grain boundaries, and because of the different crack initiation locations, the final crack has a meandering form. Although the grain boundaries were clearly the weakest part of the structure, the occurrence of slip lines (Fig. 3b) indicated that the grains themselves also deformed. Side cracks

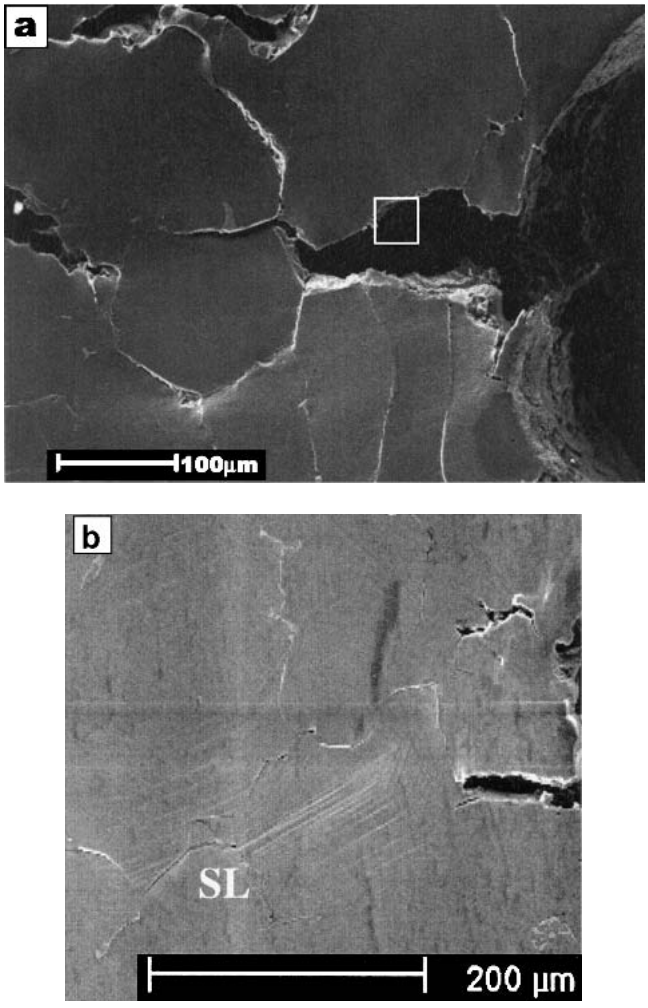

Fig. 3 Tensile deformation (direction: ↕) in SEM at 500 °C. **(a)** Cracks initiate at different locations and grow towards each other. Square: detail shown in Fig. 4. **(b)** Slip lines (SL)

were also formed, but they stopped growing when the stress was relieved by propagation of the main crack. No liquid is present at 500 °C, but when a crack is formed, solid bridges initially form the connection between the sides of the crack and they flow in a ductile manner during separation (Fig. 4).

3.3. Observation of Hot Tears in an Industrial Ingot

The cracking surface of hot tears in one of the AA5182 ingots of the industrial casting experiments was investigated by SEM. The grain size is ca. 135 μm. Many side cracks are present and the hot tear follows the grain boundaries (Fig. 5). Part of the grain boundary surface was liquid at the time of fracture, as indicated by the smooth dendrite arms. The same figure shows that the grain boundary surface was not completely covered by a liquid film. The irregular marks on the grains show evidence of solid-state deformation in places where the grains were still connected.

There are large similarities between the fracture surface of the tensile specimens (Fig. 2) and the ingot hot tears (Fig. 5). Both have a similar grain size and show intergranular fracture, solid bridges, and dendrite arms covered with a liquid layer. There are also similarities between the in situ specimens and the ingot hot tears, because both show intergranular fracture and solid bridges.

4. Discussion

4.1. Hot Tearing Observations

In the tensile tests, it was observed that apart from liquid film separation, ductile failure occurred locally where solid material formed bridges across the liquid film (Fig. 2). Thus, the material behaves in a brittle manner on the large scale, whereas locally it behaves in a ductile manner. These observations are similar to the results of tensile loaded specimens of AA2024[15] and AA6063.[12] Furthermore, the data summarized in Table 1, although too limited to make a complete ductility curve, give the general picture of a steeply decreasing ductility just above the solidus temperature, a minimum around a fraction liquid of 0.04 (560 °C), and a slight increase again at higher temperatures. This is consistent with literature data.[12,14,15,24,26]

The in situ SEM observations are especially suited to study crack propagation. They show intergranular cracking and the development of solid bridges (Fig. 3 and 4). They also show that grain boundary separation occurs in three stages, as shown

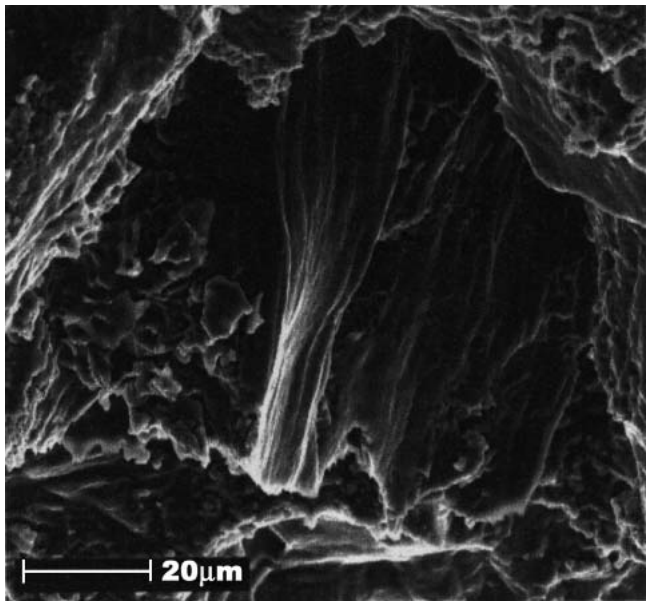

Fig. 4 SEM micrograph of fracture surface of in situ specimen. Square in Fig. 3 indicates location.

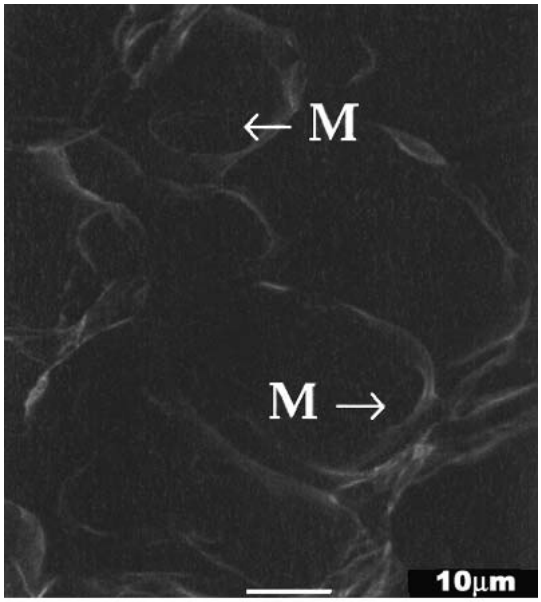

(a)

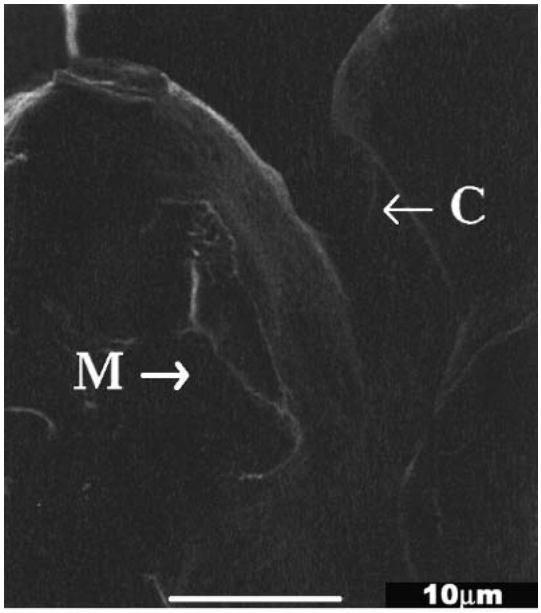

(b)

Fig. 5 SEM micrograph of the hot tear surface (in plane of paper). **(a)** Marks (M) on surface indicate solid state rupture. **(b)** Side crack with marks and capillary meniscus (C) of remaining film

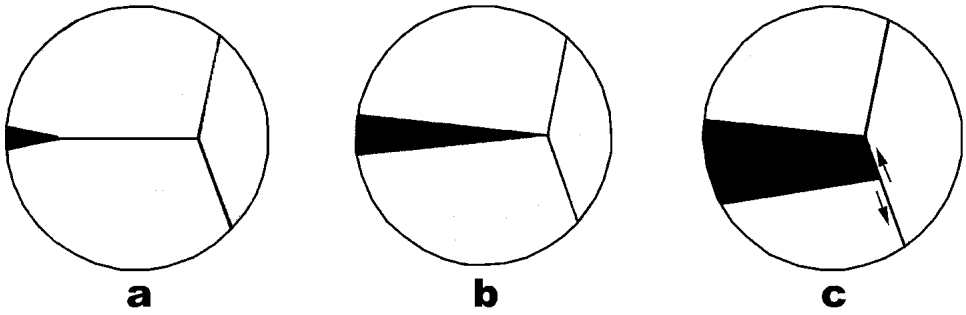

Fig. 6 Schematic drawing of three stages of grain boundary separation (tensile direction: ↕). **(a)** Separation by a wedge. **(b)** Crack arrest. **(c)** Sliding

schematically in Fig. 6. Where grain boundaries are perpendicular to the tensile direction, the crack grows by opening the grain boundary as a wedge (Fig. 6a). Upon reaching a grain boundary more or less parallel to the tensile direction, the crack arrests briefly (Fig. 6b), and then continues along one of the grain boundaries by a sliding motion (Fig. 6c).

Observations on the hot tear surface of the industrial ingot show that many features such as side cracks, liquid films, solid bridges, and grain size are similar to features observed on the fracture surfaces of the tensile specimens and the in situ SEM specimens. This indicates that tensile experiments at the semisolid state such as carried out in this study can be used to study hot tearing and to evaluate existing hot tearing criteria.

Few studies investigated hot tear surfaces in an industrial billet. In AA6063, it was shown that the fracture surfaces were covered by a fluid film and α- and β-AlFeSi particles.[13] No evidence for solid-state rupture was reported, and it was concluded that hot tearing occurred during the α- to β-phase transition. In the current study, precipitates were also observed on the crack surface, but no correlation was found between nature or number of the precipitates and tendency of cracking.

The observations in the current study are based on data from reheating tests, whereas in situ solidification tests might be more appropriate in relation to the DC casting process. These tests were described in Refs. 8, 11, 12, 14, and 25. In both the in situ solidification test and the reheating test, the microstructure will be different from that in the DC cast ingot during casting. In the in situ test, cooling conditions will be different from the conditions during DC casting, whereas in the reheating test, the cooling conditions are the same (till the test temperature), but changes may occur during cooling to room temperature, during storage, and/or during reheating. These differences will affect grain size, macrosegregation, dendrite shape, and liquid film morphology. A lower ductility is reported for in situ solidified specimens, which is attributed to the existence of thicker liquid films that persist longer because of the latent heat evolution associated with solidification.[14] Rogberg[8] observed that cooling after casting of carbon steel leads to a different macrostructure, diffusion of the low melting phases away from the grain boundaries, and equalization of the originally dendritic grain boundaries. Despite these differences between in situ solidified and reheated material, the differences with the material during DC casting are not clear. Because in situ solidification tests produce many experimental difficulties, it was decided to use the reheating tests in the current study.

4.2. Hot Tearing Criteria

Figure 7 shows the strain versus strain rate of the specimens tested in a semisolid state. It indicates that tendency for cracking is mainly a function of strain rate. This is recognized by a recent hot tearing model of Rappaz et al.[20] They calculate the pressure drop caused by separation of the dendrite arms and lack of afterfeeding caused by the restricted permeability of the mushy zone, and assume a critical pressure for cavity nucleation. Unfortunately, it is not possible to calculate the critical strain rate to attain a certain cavitation pressure, which makes it difficult to compare the model quantitatively to experimental data. The model is further developed by Braccini et al.[22] to include crack growth and deformation of the solid network. This modification makes it possible to calculate directly the strain rates at which nucleation or cavity growth occurs, which allows comparison with the experimental data. They apply a series model based on two simplified geometrical models: one for a columnar dendritic structure and one for an equiaxed dendritic structure. For an equiaxed structure, which corresponds best to the microstructure in our specimens, the following expressions were derived:

$$\dot{\varepsilon} = \left(1 - \frac{e}{h}\right)\left[\frac{\lambda - a}{\lambda}\left(\frac{2/3p_c - p_m}{K(T, f_S)}\right)\right]^{1/m} + \frac{e}{h}\frac{2\kappa}{(\lambda - a)^2}\frac{p_c}{\eta_L} \quad \text{(Eq 1)}$$

with

$$\kappa = \frac{e^2}{32}(1 - f_S)(f_S^c - f_S)^{1.3} \quad \text{(Eq 2)}$$

where $\dot{\varepsilon}$ is the critical strain rate for hot tearing, e is the liquid film thickness, h is the gauge length, λ is half the grain size, a is the length of the tear, p_c is the cavitation pressure, p_m is the metallostatic pressure, K is a constitutive parameter that is a function of the temperature T and the fraction solid f_S, m is the strain rate sensitivity, κ is the permeability of the mushy zone, η_L is the viscosity of the liquid, and f_S^c is the solid fraction at which the liquid network becomes disconnected. The right-hand side of Eq 1 is divided in two parts, the first describing the behavior of the solid skeleton and the second describing the liquid flow, calculated with Darcy's law. The parameters used are given in Table 2. Instead of assigning to h a macroscopic quantity (gauge length), we prefer to take a microscopic quantity corresponding to the distance where the local disturbance

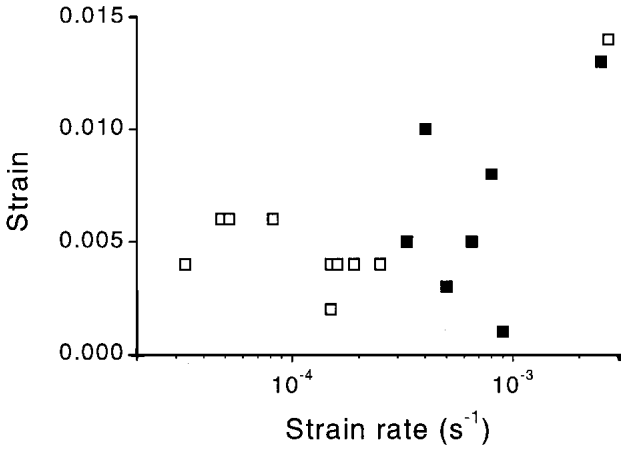

Fig. 7 Strain versus strain rate of specimens tested in semisolid state: (□) nonfractured specimens, (■) fractured specimens

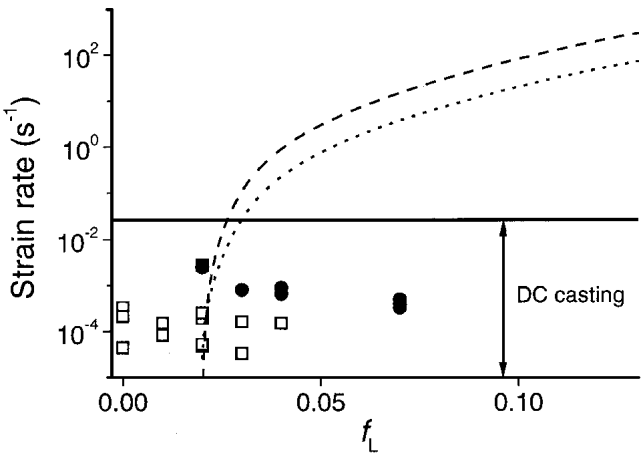

Fig. 8 Comparision of experimental data with the model for cavity nucleation (···) and growth (– – –) in AA5182 with an equiaxed structure. Nonfractured specimens (□) and fractured specimens (●). Range of relevant strain rates during DC casting is indicated.

Table 2 Parameters Applied in Eq 1 and 2 for the Calculation of Cavity Nucleation and Growth in AA5182

Parameter	Value/Expression Applied	Reference
e	$f_L \cdot \lambda$	[22]
h	350 μm (3 × grain size)	
λ	60 μm	
a	0 μm, 30 μm	
p_c	$4/e \cos(\theta)\sigma_{LV}$	[22]
θ	6°	[22]
σ_{LV}	0.914 J/m^2	[22]
p_m	0 Pa	
K	Calculated from constitutive parameters	[33]
m	0.3	[33]
η_L	0.001 Pa.s	[22]
f_s	Calculated from Alstruc	[30-32]
f_s^c	0.98	[20,22]

vanishes and estimate the distance equal to three times the grain radius. The metallostatic pressure is set equal to zero because there is no macroscopic afterfeeding in the experiments. With hot tear length *a* equal to zero, Eq 1 gives the critical strain rate for hot tear nucleation. For a certain hot tear length *a*, Eq 1 gives the minimum strain rate at which the hot tear will propagate. For *K* we used the constitutive description for the mushy zone, which is based on tensile tests and takes into account the liquid film geometry,[33] whereas in Ref. 22 the constitutive equation was based on shear experiments.

The minimum strain rates for both nucleation and growth are given in Fig. 8. Except for the highest solid fractions, the result is dominated by the liquid flow part in Eq 1. The critical strain rate for growth is higher than for nucleation, which means that the first is important for hot tearing. The critical strain rate increases with increasing liquid fraction because of the higher permeability of the mush.

The experimental data from Table 1 are also shown in Fig. 8. It is observed that there is a one to four orders of magnitude difference between the model and the experimental data. Furthermore, in contrast to the model, the experimental data show a decreasing strain rate with increasing liquid fraction. These differences are explained as follows. First, the model is highly sensitive to some parameter values used. For instance, uncertainties in the chosen fraction solid at which the liquid network becomes fragmented (f_S^c) strongly influence the maximum solid fraction at which the model is valid. Second, in the tensile test, macroscopic feeding is not provided and local flow is restricted. Therefore, the critical strain rate will be lower. Because the strength of the solid network is measured rather than the effect of feeding, the critical strain rate will decrease with increasing liquid fraction. Both the RDG model[20] and the series model of Braccini[22] take into account the deformation of the solid phase, but the critical strain rate in both models is almost exclusively determined by afterfeeding. In future models, solid bridges should be better accounted for, e.g., by using a parallel model rather than a series model for the microstructure. The experimental setup should have the possibility for afterfeeding, such as in an apparatus recently developed by Instone et al.[25] In addition, the model does not account for healing mechanisms other than fluid flow. For instance, diffusion is very fast in the liquid film and will contribute to strain accommodation in the final stage of solidification.

Despite the difficulties in linking the existing models with the experimental data, both give information relevant to hot tearing during DC casting. The model indicates the importance of fluid flow, whereas the experiments illustrate the role of solid bridges. It is concluded that with the current knowledge, it is possible to rank alloys with respect to their tendency for hot tearing but there is still no constitutive description of the hot tearing mechanism.

5. Conclusions

Microstructural investigations of cracking induced in the semisolid temperature range indicate that cracking in AA5182 starts at any weak spot such as a pore or partially liquid grain boundary, follows almost exclusively the grain boundaries, and occurs by a combination of fluid film separation and rupture of solid bridges. This leads to brittle behavior on the large scale,

although locally, deformation can be very ductile. Similarities between hot tears in the industrial ingot and cracked specimens indicate that important aspects of hot tearing during casting can be simulated by tensile experiments at semisolid temperatures.

The validity of the current hot tearing models is restricted to relatively high liquid fractions ($f_L > 0.1$) because the models do not take into account the presence of solid bridges. Experiments indicate that hot tearing occurs at a strain rate of about 10^{-3} s^{-1}. This value should be regarded as a minimum value for hot tearing because during casting, afterfeeding will (partly) compensate the straining of the mush.

Acknowledgments

This research was carried out as part of the EMPACT Brite-Euram project (BRPR-CT95-0112). Funding by the European Community is greatly acknowledged. Mr. G.-U. Grün (VAW, Germany) is thanked for performing the industrial casting experiment and providing the material for this study. The authors very much appreciate the use of the experimental equipment at Hydro Aluminum R&D (Norway) and thank Mr. T. Iveland (Hydro Aluminum a.s., Norway) for technical assistance. Mr. C. van Dijk (University of Groningen, The Netherlands) is thanked for his help with the in situ SEM experiments.

References

1. H.F. Bishop, C.G. Ackerlind, and W.S. Pellini: "Metallurgy and Mechanics of Hot Tearing," *AFS Trans.,* 1952, *60*, pp. 818-33.
2. W.S. Pellini: "Strain Theory of Hot Tearing," *Foundry,* 1952, *80*, pp. 125-99.
3. J.C. Borland: "Generalized Theory of Super-Solidus Cracking in Welds (and Castings)," *Br. Welding J.,* 1960, *7*, pp. 508-12.
4. S.A. Metz and C. Flemings: "A Fundamental Study of Hot Tearing," *AFS Trans.,* 1970, *78*, pp. 453-60.
5. U. Feurer: "Mathematisches Modell der Warmrissneigung von binären Aluminiumlegierungen," *Giessereiforschung,* 1976, *28*, pp. 75-80 (in German).
6. T.W. Clyne and G.J. Davies: "Comparison Between Experimental Data and Theoretical Predictions Relating to Dependence of Solidification Cracking on Composition" in *Proceedings of the Conference on Solidification and Casting of Metals*, University of Sheffield, Sheffield, UK, 1979, pp. 275-78.
7. F. Matsuda, H. Nakagawa, S. Katayama, and Y. Arata: "Weld Metal Cracking and Improvement of 25%Cr-20%Ni (AISI 310S) Fully Austenitic Stainless Steel," *Trans. Jpn. Weld. Soc.,* 1982, *13*, pp. 115-32.
8. B. Rogberg: "An Investigation on the Hot Ductility of Steels by Performing Tensile Tests on 'In Situ Solidified' Samples," *Scand. J. Met.*, 1983, *12*, pp. 51-66.
9. J. Campbell: *Castings*, Butterworth-Heinemann, Oxford, UK, 1991, 288 pp.
10. G.K. Sigworth: "Hot Tearing of Metals," *Can. Met. Q.,* 1996, *35*, pp. 1053-62.
11. J.A. Spittle and A.A. Cushway: "Influences of Superheat and Grain Structure on Hot-Tearing Susceptibilities of Al-Cu Castings," *Met. Technol.,* 1983, *10*, pp. 6-13.
12. L. Ohm and S. Engler: "Festigkeiteigenschaften erstarrender Randschalen aus Aluminiumlegierungen," *Giessereiforschung*, 1990, *42*, pp. 149-62 (in German).
13. M.L. Nedreberg: "Thermal Stresses and Hot Tearing During DC Casting of AlMgSi Billets," Ph.D. Thesis, University of Oslo, Norway, 1991, 184 pp.
14. J.P. Boyle, D.A. Mannas, and D.W. Walsh: "The Effects of Grain Size on Hot Cracking of Welded 2014 Aluminum Alloy Rolled Rings Forgings" in *International Symposium on Physical Simulation*, D. Ferguson and J. Jacon, ed., Dynamic Systems Inc., Poestenkill, NY, 1992, pp. 165-73.
15. J.A. Spittle, S.G.R. Brown, J.D. James, and R.W. Evans: "Mechanical Properties of Partially Molten Aluminum Alloys" in *Physical Simulation of Casting, Hot Rolling and Welding*, National Research Institute for Metals, Tsukuba, Japan, 1997, pp. 81-91.
16. W.M. van Haaften, W.H. Kool, and L. Katgerman: "Microstructural Observations of Cracking in AA5182 at Semi-Solid Temperatures," *Mater. Sci. Forum,* 2000, *331-337*, pp. 265-70.
17. I. Farup, J.-M. Drezet, and M. Rappaz: "In-Situ Observation of Hot Tearing Formation in Succinonitrile-Acetone," *Acta Mater.,* 2001, *49*, pp. 1261-69.
18. B. Forest and S. Berovici: "Experimental Study of Mechanical Properties of Aluminum Alloys During Controlled Solidification: Application to Hot Tearing" in *Solidification Technology in the Foundry and Cast House,* TMS, London, UK, 1983, pp. 607-12.
19. L. Katgerman: "A Mathematical Model for Hot Cracking of Aluminum Alloys During DC Casting," *J. Met.,* 1982, *34*, pp. 46-49.
20. M. Rappaz, J.-M. Drezet, and M. Gremaud: "A New Hot-Tearing Criterion," *Met. Mater. Trans. A,* 1999, *30A*, pp. 449-55.
21. J.-M. Drezet and M. Rappaz: "Prediction of Hot Tears in DC-Cast Aluminum Billets," in *Light Metals 2001*, J.L. Anjier, ed., TMS, Warrendale, PA, 2001, pp. 887-93.
22. M. Braccini, C.L. Martin, M. Suéry, and Y. Bréchet: "Modeling of Casting, Welding and Advanced Solidification Processes" in *MCWASP IX*, P.R. Sahm, P.N. Hansen, and J.G. Conley, ed., Shaker Verlag, Aachen, Germany, 2000, pp. 19-24.
23. W.T. Lankford: "Some Considerations of Strength and Ductility in the Continuous-Casting Process" *Metall. Trans.,* 1972, *3*, pp. 1331-57.
24. B. Magnin, L. Maenner, L. Katgerman, and S. Engler: "Ductility and Rheology of an Al-4.5%Cu Alloy From Room Temperature to Coherency Temperature," *Mater. Sci. Forum,* 1996, *217-222*, pp. 1209-14.
25. S. Instone, D. St John, and J. Grandfield: "New Apparatus for Characterising Tensile Strength Development and Hot Cracking in the Mushy Zone," *Int. J. Cast Met. Res.,* 2000, *12*, pp. 441-56.
26. J.A. Williams and A.R.E. Singer: "Deformation, Strength, and Fracture Above the Solidus Temperature," *J. Inst. Met.,* 1968, *96*, pp. 5-12.
27. C.L. Martin, D. Favier, and M. Suéry: "Fracture Behavior in Tension of Viscoplastic Porous Metallic Materials Saturated with Liquid," *Int. J. Plast.,* 1999, *15*, pp. 981-1008.
28. H. Fredriksson and B. Lehtinen: "Continuous Observation of Hot Crack-Formation During Deformation and Heating in SEM" in *Proceedings of the Conference on Solidification and Casting of Metals*, University of Sheffield, Sheffield, UK, 1979, pp. 260-67.
29. W.M. van Haaften, B. Magnin, W.H. Kool, and L. Katgerman: "Thermomechanical Behavior of an AA3004 Alloy at Low Strain Rate" in *Light Metals 1999*, C.E. Eckert, ed., TMS, Warrendale, PA, 1999, pp. 829-33.
30. E.K. Jensen: Elkem Research, Norway, private communication, 2000.
31. A. Håkonsen: Hydro Aluminum, Norway, private communication, 2000.
32. A.L. Dons, E.K. Jensen, Y. Langsrud, E. Trømborg, and S. Brusethaug: "The Alstruc Microstructure Solidification Model for Industrial Aluminum Alloys," *Met. Trans. A,* 1999, *30A*, pp. 2135-46.
33. W.M. van Haaften, W.H. Kool, and L. Katgerman: "Tensile Behavior of Semi-Solid AA3104 and AA5182," *Mater. Sci. Eng. A.,* 2002, *336*(1-2), pp. 1-6.